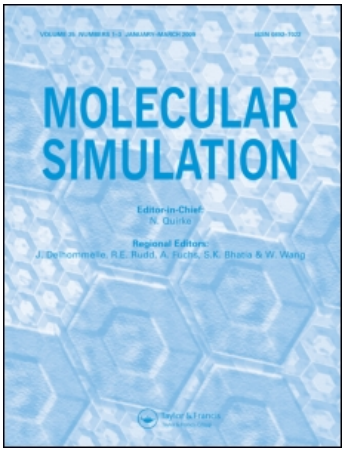

Molecular Simulation
Publication details, including instructions for authors and subscription information:
http://www.informaworld.com/smpp/title~content=t713644482

Histogram of number of particles as an indicator for 2D phase transition in adsorption of gases on graphite

L. F. Herrera[a]; D. D. Do[a]; G. R. Birkett[a]
[a] School of Chemical Engineering, University of Queensland, St Lucia, Queensland, Australia

Online publication date: 10 December 2010

To cite this Article Herrera, L. F. , Do, D. D. and Birkett, G. R.(2010) 'Histogram of number of particles as an indicator for 2D phase transition in adsorption of gases on graphite', Molecular Simulation, 36: 14, 1173 — 1181
To link to this Article: DOI: 10.1080/08927022.2010.509863
URL: http://dx.doi.org/10.1080/08927022.2010.509863

Molecular Simulation
Vol. 36, No. 14, December 2010, 1173–1181

Taylor & Francis
Taylor & Francis Group

Histogram of number of particles as an indicator for 2D phase transition in adsorption of gases on graphite

L.F. Herrera, D.D. Do* and G.R. Birkett

School of Chemical Engineering, University of Queensland, St Lucia, Queensland 4072, Australia

(*Received 18 April 2010; final version received 17 July 2010*)

Grand canonical Monte Carlo simulation is used to study the adsorption of gases with strong and weak molecular interaction on graphite. We choose nitrogen adsorption at 77 K, ethylene at 104 K, methanol at 240 K and ammonia at 300 K as model examples. The adsorption mechanism of these species can be studied by analysing the radial distribution and the 'number of particles histogram' as a function of loading. At low pressures, at which the surface is barely covered with molecules, nitrogen and ethylene adsorb in a similar manner, while ammonia and methanol show a distinct difference because of the formation of clusters, resulted from the hydrogen bonding. Small clusters are observed for methanol and larger ones for ammonia, which is in agreement with the fact that hydrogen bonding is more significant in ammonia than in methanol. Analysis of the number of particles distribution can identify 2D phase transition as a sudden shift of the peak in the number histogram as exemplified with the adsorption of ethylene at 104 K and ammonia at 300 K.

Keywords: molecular simulation; condensation; nitrogen; ethylene; methanol

1. Introduction

The adsorption equilibrium of fluids is governed by the interaction between fluid molecules and the solid atoms. These interactions are a complex function of variables such as temperature, pressure, pore size and surface topology. Molecular simulation has become the preferred method of choice to study adsorption because it can simulate adsorption at the molecular scale and can account for these variables more directly. It has been seen that molecular simulation can reproduce the features of the adsorption equilibrium when proper potential models for the fluid–fluid and fluid–solid interactions are used. Since its first presentation by Metropolis et al. [1] in 1953, molecular simulation has been widely applied to study the effects of variables such as molecular fluid shape [2–4], geometry of the solid surface [5–7] and functional groups [8–10] on the adsorption equilibrium.

In molecular simulation, most studies focus on the adsorption isotherms and the isosteric heat. These are macroscopic variables which are necessary for the overall mass and energy balances. However, molecular simulation can also provide information about the microscopic characteristics of the system such as the local density distribution and the radial distribution. As a part of the microscopic study of adsorption, we propose the 'number of particles histogram' as a new means to identify the 2D condensation in the adsorption of gases on a surface. In this paper, this histogram is used to study the adsorption of gases with strong and weak molecular interaction on graphite and we highlight its main application in the determination of 2D phase transition with the study of ethylene and ammonia adsorption.

2. Simulation methodology

2.1 Fluid–fluid potential model

The potential models used in this study are the models proposed by Potoff and Siepmann [11], Kristof et al. [12], Chen et al. [13] and Wick et al. [14] for nitrogen, ammonia, methanol and ethylene, respectively. These models are written as the sum of Coulomb and Lennard-Jones (LJ) interactions.

$$u_{ij} = \sum_{a=1}^{A}\sum_{b=1}^{B}\frac{q_i^a q_j^b}{4\pi\varepsilon_0 r_{ij}^{ab}} + \sum_{c=1}^{C}\sum_{d=1}^{D}4\varepsilon_{ij}^{cd}\left[\left(\frac{\sigma_{ij}^{cd}}{r_{ij}^{cd}}\right)^{12}-\left(\frac{\sigma_{ij}^{cd}}{r_{ij}^{cd}}\right)^{6}\right], \quad (1)$$

where u_{ij} is the interaction energy between fluid molecules i and j; A and B are the number of charges on the molecules i and j, respectively; C and D are the number of LJ sites for each molecule; ε_0 is the permittivity of a vacuum; r_{ij}^{ab} is the separation between the charges a and b on molecules i and j having charges q_i^a and q_j^b, respectively; r_{ij}^{cd} is the separation

*Corresponding author. Email: d.d.do@uq.edu.au

ISSN 0892-7022 print/ISSN 1029-0435 online

DOI: 10.1080/08927022.2010.509863
http://www.informaworld.com

between the LJ site c on molecule i and the LJ site d on molecule j with a combined LJ well depth of ε_{ij}^{cd} and a combined LJ collision diameter of σ_{ij}^{cd}. The combined well depth and collision diameters are given by the Lorentz–Berthelot (LB) mixing rule

$$\varepsilon_{ij}^{cd} = \sqrt{\varepsilon_i^c \varepsilon_j^d}, \tag{2a}$$

$$\sigma_{ij}^{cd} = 0.5\left(\sigma_i^c + \sigma_j^d\right). \tag{2b}$$

The nitrogen model has two LJ sites, one at each atom separated by 0.11 nm ($\varepsilon/k_b = 36$ K and $\sigma = 0.331$ nm). There are three partial charges on the molecule oriented along the same axis as the LJ sites with a single positive charge at the centre ($+0.964e$) and two negative charges ($-0.482e$) at the same positions as the LJ sites. The ammonia molecule is a triangular-based pyramid with the nitrogen at its apex and the hydrogen atoms on the base. The separation between the nitrogen site and the hydrogen sites is 0.10124 nm and the angle formed by two hydrogen sites and the nitrogen site is 106.68°. The nitrogen atom has an LJ site ($\sigma_{N-N} = 0.3385$ nm and $\varepsilon_{N-N}/k_b = 170$ K) and a partial charge of $-1.035e$. For each of the hydrogen atoms, there is a partial charge of $+0.345e$. These parameters were adjusted to reproduce ammonia vapour–liquid equilibria above 281 K [12]. However, Birkett and Do [8] showed that this model also gives an acceptable vapour pressure at 240 K. They obtained simulation results which are in good agreement with experimental isotherms on highly graphitised carbon blacks from Spencer et al. [15], and Avgul and Kiselev [16].

The model used for methanol is the 'TraPPE–UA' [13], which was optimised for the vapour–liquid equilibria of methanol. Originally, this model included the effects of bond angle bending, however it is not considered here. This model has two LJ sites, one for the CH_3 group ($\sigma_{CH_3-CH_3} = 0.375$ nm and $\varepsilon_{CH_3-CH_3}/k_b = 98.0$ K) and the other for the oxygen ($\sigma_{O-O} = 0.302$ nm and $\varepsilon_{O-O}/k_b = 93.0$ K). There are three charges, one on methyl group ($+0.265e$) and the other two are on hydrogen ($+0.435e$) and oxygen ($-0.700e$). The carbon–oxygen bond length is 0.1430 nm and the oxygen–hydrogen bond length is 0.0945 nm. The angle formed by COH is 108.5°. This model was used by Birkett and Do [9] to give a good agreement between simulated and experimental isotherms for the case of graphitised carbon black. We use the potential model proposed by Wick et al. [14] for the simulation of ethylene. This model has two LJ sites ($\sigma_{f-f} = 0.3675$ nm and $\varepsilon_{f-f}/k_b = 85.0$ K) separated by a distance equal to the carbon–carbon double bond length (0.133 nm). These molecular parameters are effective in the sense that they embed the quadrupole effects of ethylene [17], and this model of Wick et al. has been shown to describe well the adsorption of ethylene at different conditions [18,19].

2.2 Solid–fluid potentials

The simulation box used for this study is the region enclosed by the dash-dotted line in Figure 1. It is characterised by a height of $H = 3.2$ nm with the length of the simulation cell, L, in the x and y axes equal to 4.5 nm. The simulation box is bound in the z-axis by a homogeneous carbon surface and a hard wall. The solid–fluid interaction potential is calculated with the Steele 10–4–3 potential equation [20]:

$$u_{i,\mathrm{surf}} = \sum_{a=1}^{A} 2\pi\rho_s \varepsilon_{is}^a \left(\sigma_{is}^a\right)^2 \left[\frac{2}{5}\left(\frac{\sigma_{is}^a}{z_i^a}\right)^{10} - \left(\frac{\sigma_{is}^a}{z_i^a}\right)^4 - \left(\frac{{\sigma_{is}^a}^4}{3\Delta\left(z_i^a + 0.61\Delta\right)^3}\right)\right], \tag{3}$$

where $u_{i,\mathrm{surf}}$ is the interaction energy between a molecule and the surface; ρ_s is the surface density of the carbon in graphite ($38.2\ \mathrm{nm}^{-2}$); Δ is the separation distance between two adjacent graphene layers (0.3354 nm); z_i^a is the distance from the surface to LJ site a on molecule i; and σ_{is}^a and ε_{is}^a are the LJ parameters between the fluid and the surface. For nitrogen, ammonia and methanol, the combined LJ parameters were calculated by Equations (2a) and (2b), while for ethylene, the well-depth interaction energy is adjusted with the solid–fluid interaction parameter ($k_{sf} = -0.05$) as $\varepsilon_{is}^a = (1 - k_{sf})\sqrt{\varepsilon_i^a \varepsilon_s}$, where ε_{is}^a is the well depth between the LJ site a of the molecule i and the surface ($\sigma_s = 0.34$ nm and $\varepsilon_s/k_b = 28.0$ K). This correction is to give a good description of the adsorption isotherm at low loadings.

2.3 Monte Carlo simulation

Grand canonical Monte Carlo simulations were performed for each fluid at the temperatures and pressures given in Table 1. The chemical potential used in the simulation was the ideal chemical potential at the pressure reported. This is because the low-pressure range used in the simulations and ideal gas is essentially obeyed. Each isotherm point was equilibrated using 5×10^6 to 1×10^8 attempted trial moves depending on the number of particles and the point on the isotherm. Ensemble averages were taken using 5×10^6 to 1×10^8 attempted trial moves. The probability of an

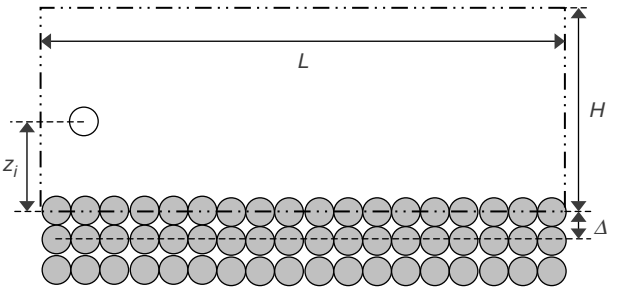

Figure 1. Schematic diagram of the simulation box.

Table 1. Set temperature, vapour pressure and pressure ranges of simulation.

Molecule	Temperature (K)	Vapour pressure (kPa)	Range of pressure (kPa)
Nitrogen	77	101.3300	7×10^{-5}–102.6
Ethylene	104	0.1206	1×10^{-7}–1.1×10^{-1}
Methanol	300	16.9000	1×10^{-3}–12.0
Ammonia	240	107.0000	0.01–80.0

attempted insertion and deletion was the same and it was set to achieve a successful insertion once every 50 attempted moves. When this was not achievable due to low-insertion probabilities, the probability of an attempted insertion was limited to five times that of an attempted move.

The local density, perpendicular to the surface, and the radial distribution [21] were calculated with Equations (4) and (5), respectively, where ρ_z is the local density; $\langle \Delta N_{z+\Delta z} \rangle$ is the ensemble number of particles in the region from $z - 0.5(\Delta z)$ to $z + 0.5(\Delta z)$, with Δz equal to 0.01 nm; V is the total volume; $\langle N \rangle$ is the ensemble number of particles; δ is the delta function; and r is the distance from a particle i in which the radial density is estimated and r_{ij} is the distance between particles i and j.

$$\rho_z = \frac{\langle \Delta N_{z+\Delta z} \rangle}{L_x L_y \Delta z}, \tag{4}$$

$$g(r) = \frac{V}{\langle N \rangle^2} \left\langle \sum_i \sum_{j \neq i} \delta(r - r_{ij}) \right\rangle. \tag{5}$$

3. Results and discussion

3.1 Adsorption of ethylene and nitrogen

The comparison between simulation results and the experimental adsorption isotherm (taken from Kruk et al. [22]) for nitrogen at 77 K is presented in Figure 2(a). The simulation results underestimate the experimental data at low pressures. This result was expected as the solid–fluid binary interaction parameter to approximate the deviation from the LB rule is not included [23]. However, over the range of higher pressures, this effect is reversed and the simulation overestimates the amount adsorbed. The comparison of simulated and experimental results for ethylene adsorption at 183 K is shown in Figure 2(b). At 183 K, the simulation results agree well with the experimental data from Avgul and Kiselev [16] for all ranges of pressure. Similar results were found by Do and Do [18] for a wider range of temperatures. Therefore, there is a good level of confidence to apply this model to simulate adsorption at 104 K. The simulation results of ethylene at 104 K are shown in Figure 2(b). At this temperature, ethylene shows a Henry law behaviour for reduced pressures up to 1.66×10^{-4} (not shown). At a reduced pressure equal to 3.7×10^{-4}, the first 2D phase transition is observed, followed by a slow increase in the amount adsorbed. This represents the compression of the monolayer. Over the high-pressure region, we observe a second 2D phase transition at a reduced pressure of 6.3×10^{-1}, which is due to the formation of the second layer above the surface. We also observe that this sudden formation of the second layer is associated with a small sharp increase in the density of the first layer, which is shown in Figure 3(b).

The local density distributions for nitrogen and ethylene are shown in Figure 3(a), (b), respectively.

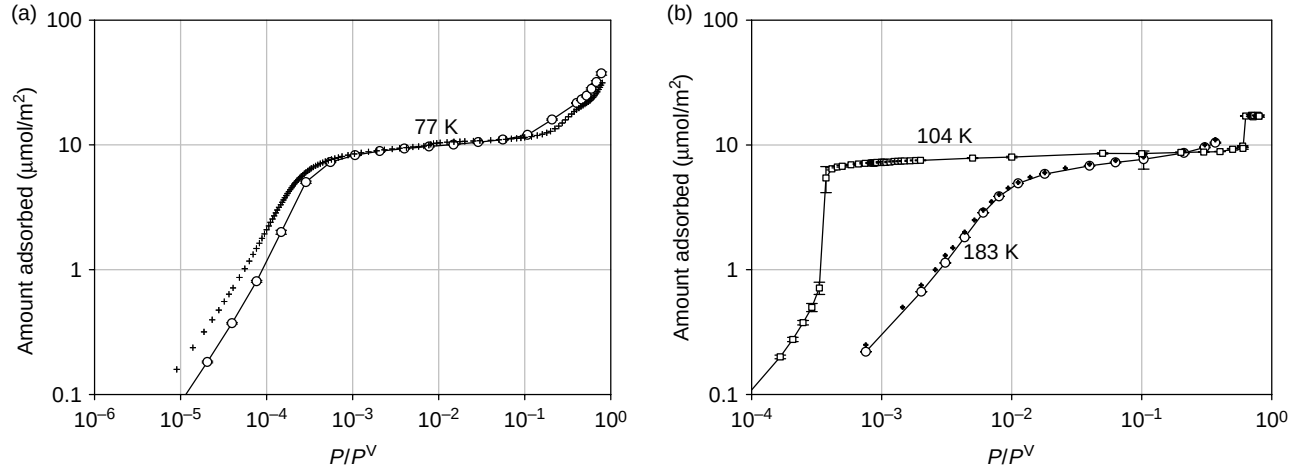

Figure 2. Adsorption isotherms for (a) nitrogen and (b) ethylene at different temperatures. Experimental data are represented by open circles, while simulation results by dark crosses. Experimental data for ethylene at 104 K are not available.

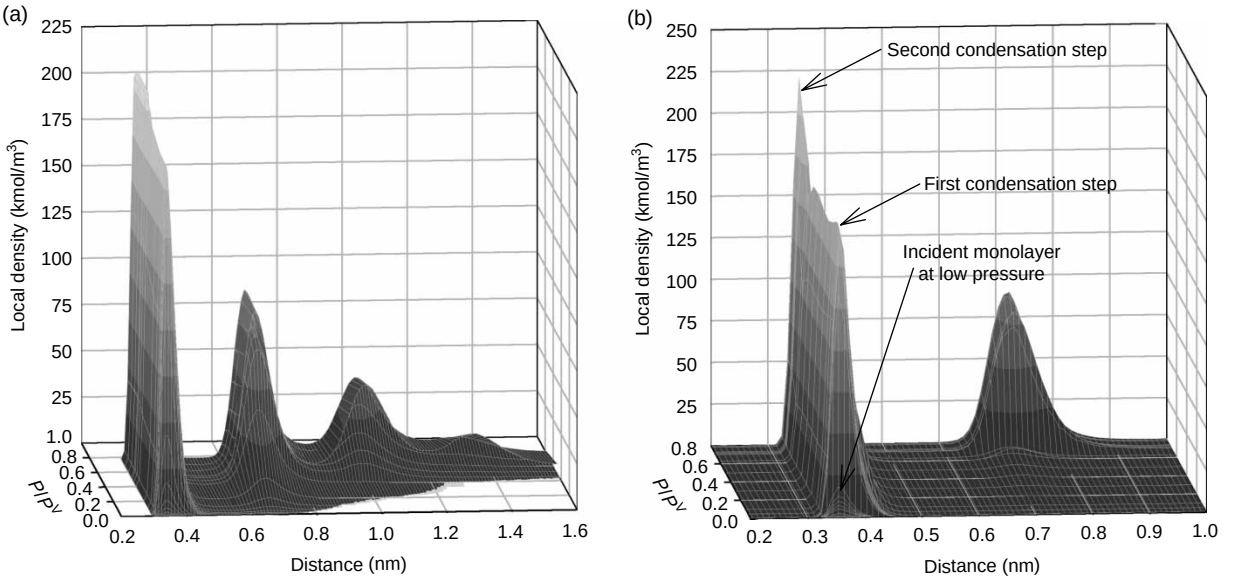

Figure 3. Density distribution perpendicular to the carbon surface for (a) nitrogen and (b) ethylene at 77 and 104 K, respectively.

Nitrogen shows a gradual build-up of a first layer at low pressures. At high pressures, there are up to four layers on the surface. In the case of ethylene in Figure 3(b), we observe a sudden change in the local density of the first layer, indicating a 2D phase transition. At high pressures, a second 2D phase transition is observed in the second layer, as well as an associated small jump in the first layer. Without this investigation of the local density distribution, the jump in the adsorption isotherm in Figure 2(b) might be thought to be resulted purely from the formation of the second layer above the surface.

To compare the molecule distribution between nitrogen and ethylene, the radial distributions of these two species were calculated at reduced pressures of 7.64×10^{-5} and 3.3×10^{-4}, respectively. The pressure points were selected to compare the molecule distribution in the first layer of ethylene before the first condensation and that for nitrogen at the same adsorbed amount ($0.7\,\mu mol/m^2$). The results are presented in Figure 4. It shows a larger peak for ethylene than that for nitrogen. It indicates that at low pressures, ethylene molecules have a greater tendency to associate than nitrogen.

To further understand the cluster formation of ethylene at 104 K, we construct a histogram of the number of particles in the simulation box during the course of simulation. This is called the 'number of particle distribution' and it gives the fraction of configurations at a given number of molecules. To characterise the number of particles distribution, the four statistical moments were calculated (mean, standard deviation, skewness and kurtosis) and we compare the third and fourth moments of the number of particles distribution with that of the normal distribution. In the case of a normal distribution, the skewness is zero. A positive or negative value of the skewness means that there is an asymmetric tail extending towards positive or negative values, respectively. Kurtosis is a measure of the significance of the tail. It is zero for the case of a normal distribution. Distributions with a positive kurtosis value are characterised by 'heavier' tails compared with the normal distribution, while if this value is negative the tails are 'lighter'.

The number of particles distribution for nitrogen at 77 K is shown in Figure 5(a). Qualitatively, nitrogen shows distributions similar to the normal distribution for all pressures. As the pressure increases, the histogram is wider and displaced to the right due to the increase in the number of particles in the simulation box. This is reflected in the

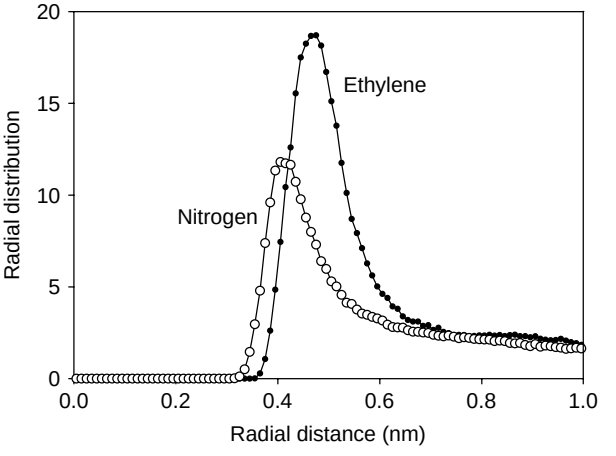

Figure 4. Radial distribution for nitrogen (white circles) and ethylene (black circles) at 7.64×10^{-5} and 3.3×10^{-4} reduced pressure. The radial distribution is calculated between centres of mass of two different molecules.

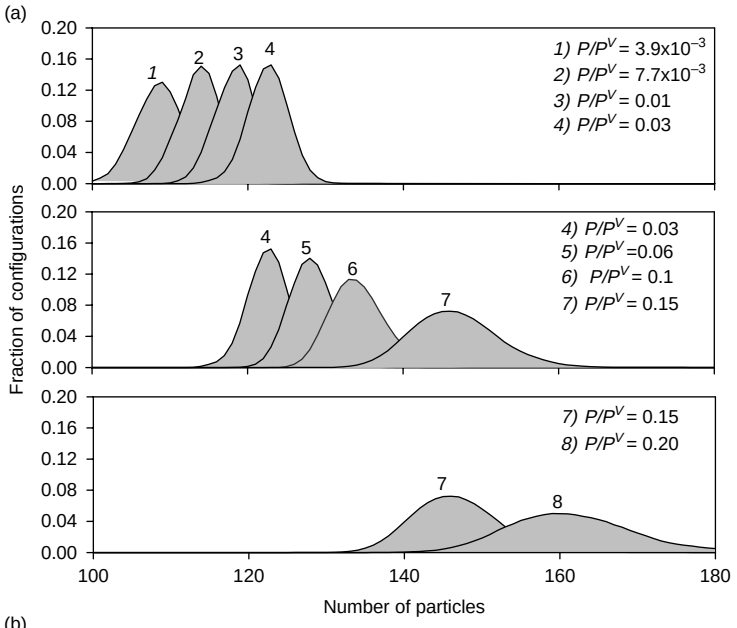

Point	Mean	Std. Dev.	Skewness	Kurtosis
1)	108.61	3.11	–0.032	0.020
2)	113.76	2.67	–0.116	–0.069
3)	118.37	2.61	–0.104	–0.128
4)	122.59	2.63	–0.078	0.111
5)	128.19	2.85	0.150	0.020
6)	134.25	3.64	0.482	0.472
7)	146.97	5.51	0.325	0.101
8)	161.59	8.17	0.444	0.345

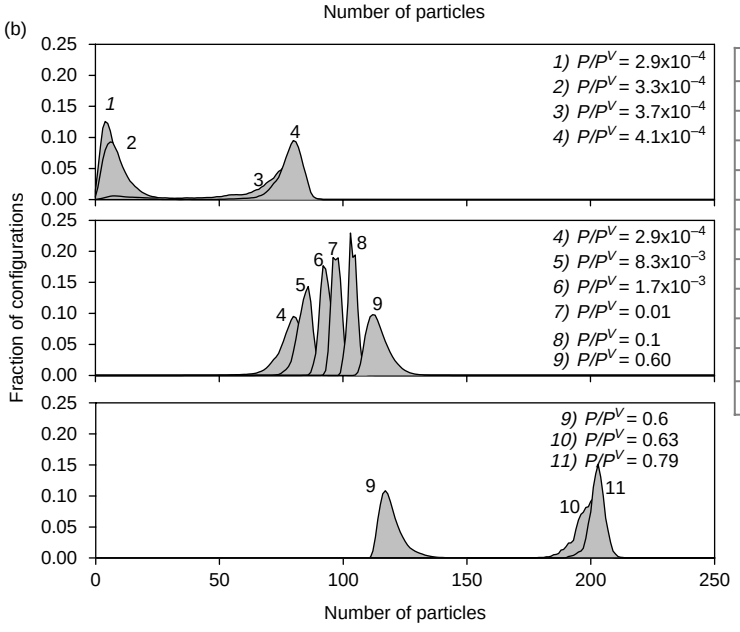

Point	Mean	Std. Dev.	Skewness	Kurtosis
1)	6.07	3.73	1.213	2.517
2)	8.69	5.15	1.077	1.370
3)	66.12	19.96	–1.775	2.262
4)	78.44	5.37	–1.428	4.234
5)	84.48	3.02	–0.594	0.726
6)	92.85	2.21	0.079	–0.033
7)	97.33	1.77	0.013	–0.590
8)	103.85	1.78	0.020	–0.114
9)	114.25	4.54	0.911	1.106
10)	198.11	4.71	–0.745	0.693
11)	202.59	3.11	–0.415	1.045

Figure 5. Number of particles histogram for (a) nitrogen at 77 K and (b) ethylene at 104 K. Note the different scale in the number of particles axes between (a) and (b).

increase in the mean and standard deviations with pressure. The skewness and kurtosis also change; at low pressures, these two values are close to zero, meaning that the distributions are close to the normal distribution. At high pressures, these two values increase, resulted from the spreading. The histogram for ethylene in Figure 5(b) shows that the distribution changes drastically with pressure. At low pressures (before the 2D phase transition), the distribution numbers 1 and 2 show a non-normal distribution with a tail extending to the right. At the reduced pressure, about 3.5×10^{-4}, where the 2D phase transition takes place, there is a sudden jump in the adsorption density and the mean increases from 8.69 to 66.14 particles for histogram numbers 2 and 3, respectively. In contrast to the histogram number 2, the skewness of the histogram number 3 is negative. This displacement and the sign change in skewness from positive to negative and vice versa can be viewed as the characteristics of a 2D phase transition. Another interesting feature in the family of ethylene histograms is observed with the distribution numbers 4–9. For these histograms, it is seen that as the pressure increases from the condensation pressure, the distribution is closer to the normal Gaussian shape. Take the histogram number 6 as an example, the third and fourth moments are close to zero. As pressure is increased even

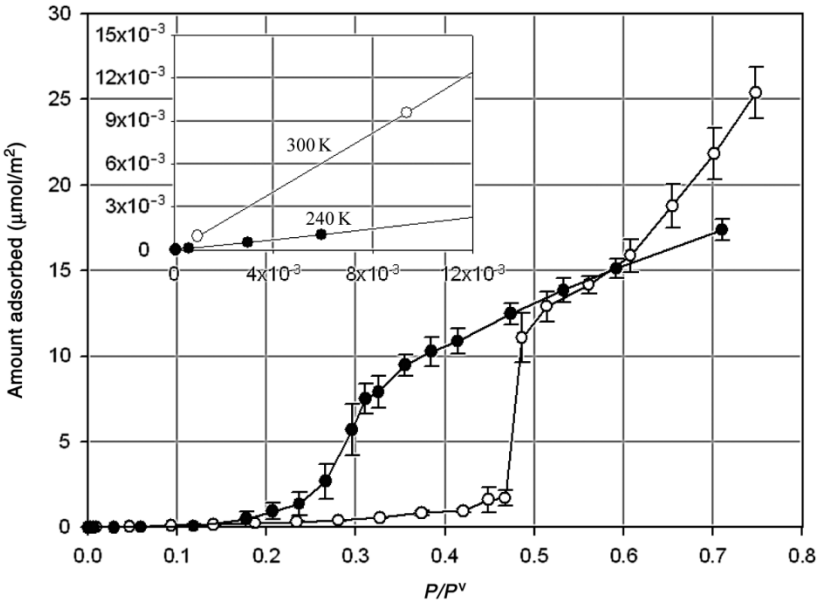

Figure 6. Adsorption of methanol at 300 K (black circles) and ammonia at 240 K (white circles).

further, we see another 2D phase transition (due to the formation of the second layer), and the characteristics of a 2D phase transition are once again reflected in:

(1) the sudden increase in the mean and
(2) the change in skewness from a positive to negative value.

This is seen in the histogram numbers 9–11 in Figure 5(b).

3.2 Adsorption of gases with strong molecular interaction

Figure 6 shows the isotherms of ammonia and methanol at 240 and 300 K, respectively. It shows that at very low pressures, the amount of ammonia adsorbed is larger than that of methanol (see the inset of Figure 6), which is due to the adsorption temperature used for each species. At moderate pressures, the methanol isotherm shows a smoother uptake while ammonia has an insignificant adsorption until the reduced pressure reaches 0.48 at which a sharp change in the adsorption amount is observed. This behaviour has also been observed experimentally by Avgul and Kiselev [16] at 195 K.

Snapshots are useful for visualising the 'instant' configurations of adsorbed molecules on the surface, even though they are only one configuration out of the numerous configurations that are realised during the course of simulation. Figure 7 shows a number of typical snapshots of ammonia at a reduced pressure of 0.47 and those of methanol at a reduced pressure of 0.23. These snapshots indicate a wide variation of adsorption density at a given pressure. It can be seen that methanol molecules have a tendency to form ring structures (clusters of four and five molecules) [9] at all loadings. In contrast, ammonia shows a tendency to form large clusters without any particular pattern. The formation of ring structures for methanol is due to the favourable hydrogen bonding among methanol

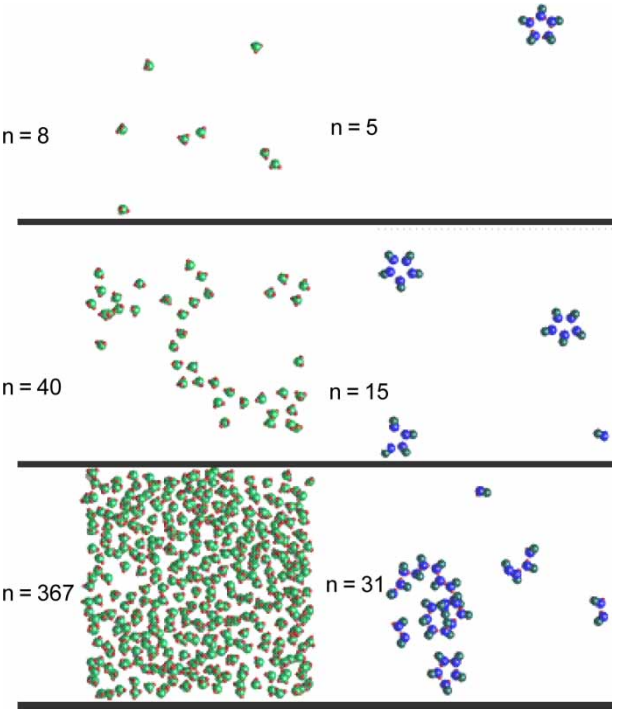

Figure 7. Snapshots of ammonia (left) at $P/P^V = 0.47$ and methanol (right) at $P/P^V = 0.23$.

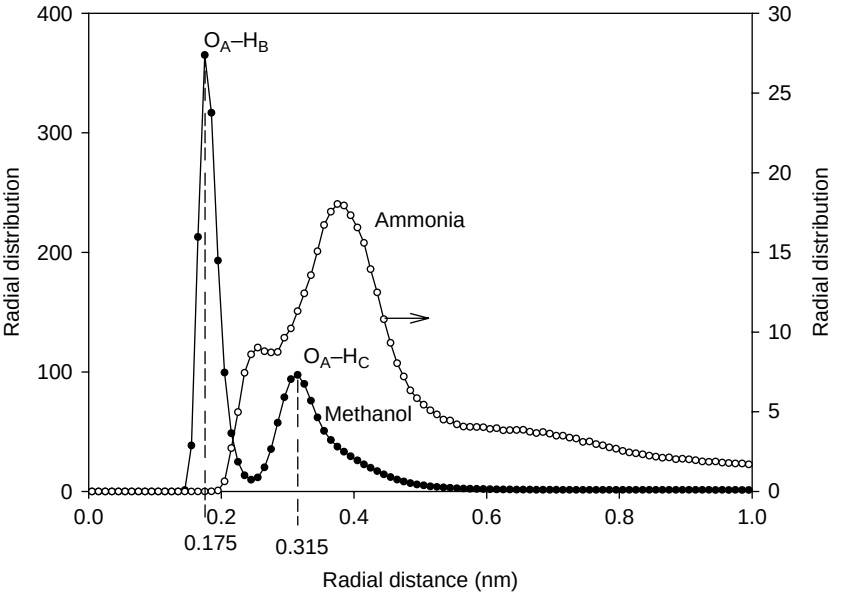

Figure 8. Radial distributions of methanol at $P/P^V = 0.23$ (black circles) and ammonia at $P/P^V = 0.47$ (white circles). For methanol, the distribution is between the oxygen of one molecule and the hydrogen of another, for ammonia the distribution is between the nitrogen of one molecule and the hydrogen of another.

molecules and these clusters are parallel to the surface to maximise the solid–fluid interaction. The structure of methanol makes it amenable to form a 2D cluster parallel to the surface. On the other hand, ammonia has a pyramid structure that is not as favourable for the formation of a 2D ring structure that possesses both strong hydrogen bonding and good solid–fluid interaction.

To confirm the above arguments, we consider in Figure 8 the radial distributions of methanol and ammonia at the same pressures as used in Figure 7. The patterns of these two radial distributions are distinctly different. The well-defined first peak of methanol confirms its strong tendency to form small clusters as was observed in Figure 7. In the case of ammonia, the first peak in the nitrogen–hydrogen radial distribution is lower than the oxygen–hydrogen peak for methanol. The more diffuse peak in the nitrogen–hydrogen radial distribution for ammonia is because the nitrogen of one molecule interacts with three hydrogen atoms of another molecule, while in the case of methanol, there is only one interaction between the oxygen of one molecule and the hydrogen of another molecule. From the radial distribution, we can confirm the 2D configuration of four methanol molecules as schematically shown in Figure 9. The first peak in the methanol radial distribution is between the oxygen of molecule A and the hydrogen of molecule B (O_A–H_B), while the second peak is between O_A and the hydrogen of molecule C (O_A–H_C). The second peak of methanol's radial distribution can be easily proved from the geometrical configuration of this particular 2D configuration (Figure 9). The distance $|O_A - H_C|$ is calculated by $(d_1 + l_{OH})^2 + d_1^2 = d_2^2$, where d_1, l_{OH} and d_2 are given in Figure 9.

Figure 10 shows the number of particles histogram for methanol. It can be seen that the histogram is gradually shifted to the right as the pressure increases. There is no evidence of any 2D phase transition step, which is similar to what was observed earlier with nitrogen. However, it is clear that the shape of the histogram does not conform to a normal distribution. This is confirmed by the values of the third and fourth statistical moments. In the case of ammonia (shown in Figure 11), the expected condensation at a reduced pressure of 0.47 is seen, as well as the expected change in skewness from positive to negative

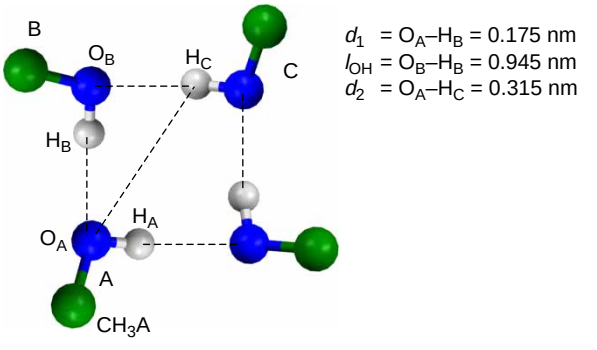

Figure 9. Representation of the 2D configuration of four methanol molecules. The white and blue spheres represent the hydrogen and oxygen atoms, respectively, while the green sphere is the methyl group.

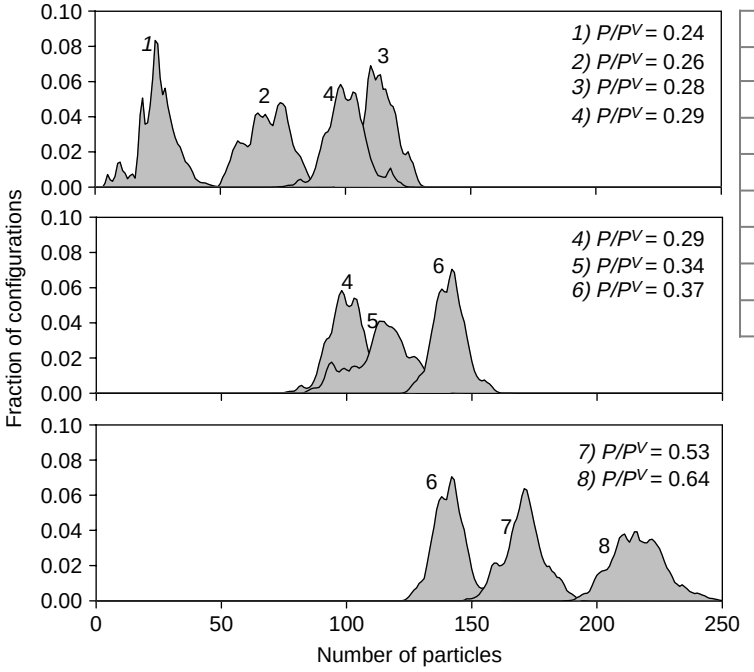

Point	Mean	Std. Dev.	Skewness	Kurtosis
1)	24.90	7.22	–0.187	0.590
2)	68.84	8.26	–0.127	–0.760
3)	100.36	7.67	0.175	0.448
4)	114.14	6.22	0.037	–0.101
5)	113.92	11.53	–0.286	–0.434
6)	141.06	6.18	0.155	0.130
7)	170.87	7.89	0.017	–0.069
8)	216.45	10.30	0.230	–0.138

Figure 10. Number of particles histogram for methanol.

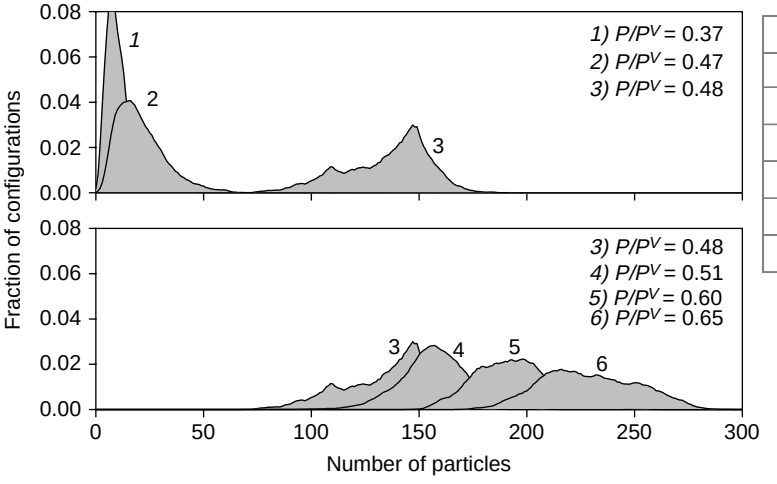

Point	Mean	Std. Dev.	Skewness	Kurtosis
1)	10.29	6.18	1.840	5.810
2)	20.77	11.14	0.955	0.850
3)	135.02	19.66	–0.576	–0.256
4)	157.42	15.95	–0.114	0.532
5)	193.50	17.77	0.338	0.038
6)	228.90	22.01	0.145	–0.661

Figure 11. Number of particles histogram for ammonia.

values. The explanation of this is similar to that presented earlier for ethylene. Additionally, the distribution of particles for higher pressures does not exhibit a normal distribution.

4. Conclusions

Monte Carlo simulations have been used to study the adsorption of ethylene (104 K), nitrogen (77 K), methanol (300 K) and ammonia (240 K) on a perfect graphite surface. The mechanisms of adsorption of these species are different as evidenced in the analysis. The nitrogen and methanol show smooth adsorption isotherms. Ethylene and ammonia show 2D phase transitions. The results show that adsorption of nitrogen and ethylene (which are the species with weak molecular interaction) behaves similarly at low pressures. In contrast, gases such as ammonia and methanol having strong interaction show a complete different mechanism of adsorption in which methanol molecules form small clusters, while ammonia shows large clusters. Finally, condensation was studied with the analysis of the histogram of particles number as a function of the loading. The non-overlapping of

two histograms and the sign change in the distribution's skewness at pressures in the near neighbourhood of condensation are suggested as an indicator for condensation. This is exemplified in the adsorption of ethylene and ammonia.

Acknowledgements

This research was made possible by the Australian Research Council whose support is gratefully acknowledged.

References

[1] N. Metropolis, A.W. Rosenbluth, and M.N. Rosenbluth, *Equation of state calculations by fast computing machines*, J. Chem. Phys. 21(6) (1953), pp. 1087–1092.

[2] G.R. Birkett and D.D. Do, *Aspects of physical adsorption on carbon black from molecular simulation*, in *Carbon Materials – Theory and Practice*, A.P. Terzyk, P.A. Gauden, and P. Kowalczyk, eds., Research Signpost, Kerala, India, 2008, pp. 351–422.

[3] J.C. Liu and P.A. Monson, *Does water condense in carbon pores?* Langmuir 21(22) (2005), pp. 10219–10225.

[4] G. Birkett and D. Do, *On the physical adsorption of gases on carbon materials from molecular simulation*, Adsorption 13(5) (2007), pp. 407–424.

[5] A. Wongkoblap, S. Junpirom, and D.D. Do, *Adsorption of Lennard-Jones fluids in carbon slit pores of a finite length. A computer simulation study*, Adsorption Sci. Technol. 23(1) (2005), pp. 1–18.

[6] A. Striolo, K.E. Gubbins, A.A. Chialvo, and P.T. Cummings, *Simulated water adsorption isotherms in carbon nanopores*, Mol. Phys. 102(3) (2004), pp. 243–251.

[7] B. Coasne and R.J.M. Pellenq, *A grand canonical Monte Carlo study of capillary condensation in mesoporous media: Effect of the pore morphology and topology*, J. Chem. Phys. 121(8) (2004), pp. 3767–3774.

[8] G.R. Birkett and D.D. Do, *Simulation study of ammonia adsorption on graphitized carbon black*, Mol. Simulat. 32(7) (2006), pp. 523–537.

[9] G.R. Birkett and D.D. Do, *Simulation study of methanol and ethanol adsorption on graphitized carbon black*, Mol. Simulat. 32(10) (2006), pp. 887–899.

[10] A. Wongkoblap and D.D. Do, *Characterization of Cabot non-graphitized carbon blacks with a defective surface model: Adsorption of argon and nitrogen*, Carbon 45(7) (2007), pp. 1527–1534.

[11] J.J. Potoff and J.I. Siepmann, *Vapor–liquid equilibria of mixtures containing alkanes, carbon dioxide and nitrogen*, AIChE 47(7) (2001), pp. 1676–1683.

[12] T. Kristof, J. Vorholz, J. Liszi, B. Rumpf, and G. Maurer, *A simple effective pair potential for the molecular simulation of the thermodynamic properties of ammonia*, Mol. Phys. 97(10) (1999), pp. 1129–1137.

[13] B. Chen, J. Potoff, and I. Siepmann, *Monte Carlo calculations for alcohols and their mixtures with alkanes. Transferable potentials for phase equilibria. 5. United-atom description of primary, secondary, and tertiary alcohols*, J. Phys. Chem. B 105(15) (2001), pp. 3093–3104.

[14] C.D. Wick, M.G. Martin, and J.I. Siepmann, *Transferable potentials for phase equilibria. 4. United-atom description of linear and branched alkenes and alkylbenzenes*, J. Phys. Chem. B 104(33) (2000), pp. 8008–8016.

[15] W.B. Spencer, C.H. Amberg, and R.A. Beebe, *Further studies of adsorption on graphitized carbon blacks*, J. Phys. Chem. 62(6) (1958), pp. 719–723.

[16] N.N. Avgul and A.V. Kiselev, *Physical adsorption of gases and vapors on graphitized carbon blacks*, Chem. Phys. Carbon 6 (1970), pp. 1–124.

[17] J. Vrabec, J. Stoll, and H. Hasse, *A set of molecular models for symmetric quadrupolar fluids*, J. Phys. Chem. B 105(48) (2001), pp. 12126–12133.

[18] D.D. Do and H.D. Do, *Adsorption of ethylene on graphitized thermal carbon black and in slit pores: A computer simulation study*, Langmuir 20(17) (2004), pp. 7103–7116.

[19] D.D. Do and H.D. Do, *Cooperative and competitive adsorption of ethylene, ethane, nitrogen and argon on graphitized carbon black and in slit pores*, Adsorption 11(1) (2005), pp. 35–50.

[20] W.A. Steele, *Physical interaction of gases with crystalline solids*, Surface Sci. 36(1) (1973), pp. 317–352.

[21] M.P. Allen and D.J. Tildesley, *Computer Simulation of Liquids*, Vol. xiii, Oxford University Press, Oxford, 1989, p. 385.

[22] M. Kruk, Z. Li, and M. Jaroniec, *Nitrogen adsorption study of surface properties of graphitized carbon blacks*, Langmuir 15 (1999), pp. 1435–1441.

[23] D.D. Do and H.D. Do, *Effects of potential models in the vapor–liquid equilibria and adsorption of simple gases on graphitized thermal carbon black*, Fluid Phase Equilibr. 236(1,2) (2005), pp. 169–177.